Natural linewidth of the 401-nm laser-cooling transition in Er I

J. J. McClelland
Electron Physics Group, Center for Nanoscale Science and Technology, National Institute of Standards and Technology, Gaithersburg, Maryland, 20899-8412 USA

(Received 31 March 2006; published 20 June 2006)

A measurement of the natural linewidth of the 401-nm $4f^{12}6s^2\ ^3\mathrm{H}_6 \rightarrow 4f^{12}(^3\mathrm{H}_6)6s6p(^1\mathrm{P}_1{}^o)\ (6,1)_7{}^o$ transition in Er I is presented. Using laser-induced fluorescence in an atomic beam, a linewidth of (35.6 ± 1.2) MHz is observed, a value that differs significantly from the literature value of 28 MHz. This measurement provides an accurate determination of an essential laser cooling parameter that plays a central role in the development of laser cooling applications using Er atoms.

DOI: 10.1103/PhysRevA.73.064502 PACS number(s): 32.70.Cs, 32.80.Pj

In laser cooling of atoms, laser light is tuned close to a strong transition between atomic energy levels, resulting in the scattering of a large number of photons and a subsequent change in momentum of the atom. A key parameter that governs nearly all aspects of laser cooling in a particular atom is the spontaneous transition rate A between the upper and lower levels of the transition. A determines a wide range of laser cooling parameters, such as saturation intensity, Rabi frequency, Doppler temperature, capture limit, and maximum deceleration [1]. It is important therefore to have accurate knowledge of the spontaneous transition rate for a specific laser cooling transition if laser cooling is to be performed.

Recently, Er has emerged as a new candidate for laser cooling with a number of attractive properties [2]. In addition to having several narrow-line transitions accessible to common lasers, which provide an opportunity for very low cooling limits, Er also has a very strong transition between the $4f^{12}6s^2\ ^3\mathrm{H}_6$ ground state and the $4f^{12}(^3\mathrm{H}_6)6s6p(^1\mathrm{P}_1{}^o)\ (6,1)_7{}^o$ excited state with a wavelength of 401 nm. This transition has proven surprisingly effective for laser cooling, and has recently been used to form a magneto-optical trap with a large number of atoms and a high density, despite the presence of optical leaks to metastable states [3]. In the process of analyzing the behavior of the Er magneto-optical trap formed with 401-nm light, it was found that measurements as a function of detuning and intensity were not consistent with the transition rate of $A = 1.73 \times 10^8\ \mathrm{s}^{-1}$ given in the literature [4]. As a result, the present study was undertaken to make a more accurate determination of this quantity.

The measurements presented here were carried out in a crossed-beam laser-induced fluorescence apparatus. The atom beam was produced in a resistively heated oven held at 1350 °C. Atoms emerged from a 1-mm-diameter aperture in the oven and were collimated by a 2-mm-diameter aperture located 450 mm in front of the oven exit. Laser light was produced by a frequency-doubled single-frequency, stabilized Ti:sapphire laser operating at 802 nm. The linewidth of the doubled laser light was approximately 2 MHz or smaller. After passing through an acousto-optical modulator, which served as a variable attenuator, the laser light was spatially filtered and expanded to a $1/e^2$ diameter of approximately 25 mm. An iris placed just before the vacuum chamber entrance window limited the beam diameter to 5 mm, creating a nominally uniform illumination region. The laser light was circularly polarized, but only because the experimental setup was adapted from a magneto-optical trap apparatus [3]. The polarization of the light does not affect the linewidth measurement. The laser and atomic beams intersected each other perpendicularly with an uncertainty of about ±3 mrad [5]. Fluorescent light was collected and imaged onto a photodiode, whose output was amplified and stored in an averaging digital oscilloscope.

A 4-GHz scan of the laser near 401 nm showed easily observable fluorescence from five isotopes of erbium. ^{164}Er, ^{166}Er, ^{168}Er, and ^{170}Er each showed single lines, spaced by about 1 GHz, and ^{167}Er showed several hyperfine lines scattered among the even isotope lines. To minimize interference from adjacent lines, measurements of the linewidth were carried out on the ^{166}Er line, which was relatively isolated from the hyperfine lines of ^{167}Er. Scans of the fluorescence line were measured at a scan rate of 294 MHz s^{-1} and averaged 64 times.

Measurements were conducted at ten different laser intensities, ranging from 8.6 to 145 W m^{-2}, and the results are shown in Fig. 1, along with fits of a Lorentzian line-shape function to the data. The range of laser intensities was chosen to eliminate any effect that power broadening might have on the linewidth measurement. With the measured value of $A = 2.2 \times 10^8\ \mathrm{s}^{-1}$, the saturation intensity $I_s = \pi hcA/(3\lambda^3)$ is 730 W m^{-2}. Thus the measured intensities were well below the level at which significant power broadening is expected. Nevertheless, since a range of intensities was investigated, the linewidth could be plotted as a function of intensity and extrapolated to find a zero-intensity value. This extrapolation is shown in Fig. 2, where the full widths at half maximum of the Lorentzian fits to the data in Fig. 1 are shown as a function of intensity, along with the least-squares-fitted line used to extrapolate to zero intensity. A linear extrapolation was used because in the limit of low intensity, the power-broadened linewidth takes the form $\Delta\nu = \Delta\nu_0[1 + I/(2I_s)]$, where $\Delta\nu_0$ is the natural linewidth and I is the laser intensity. The result of the extrapolation was a linewidth of 35.6 MHz.

The frequency calibration of the laser scan was derived from the 1.5-GHz free spectral range of a commercial scanning Fabry-Perot spectrum analyzer. Using this frequency reference, it was possible to obtain a conversion from the scan voltage of the Ti:sapphire laser to laser frequency. Recording the scan voltage simultaneously with the fluores-

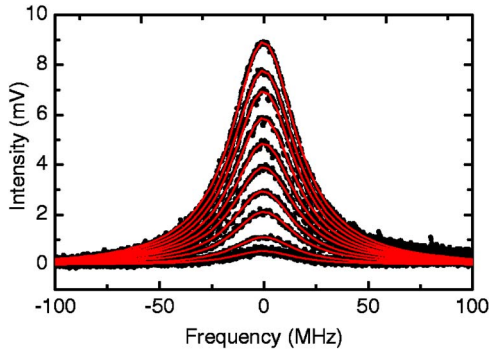

FIG. 1. (Color online) Measurements of laser-induced fluorescence of the $4f^{12}6s^2(^3H_6) \rightarrow 4f^{12}(^3H)6s6p(^1P_1^o)\ (6,1)_7^o$ transition in Er I at 401 nm. Spectra shown were obtained at incident laser intensities of 8.6, 15.6, 31.3, 45.1, 62.2, 76.6, 94.9, 110.4, 124.0, and 145.4 W m^{-2}. Solid lines (red online) indicate the fits to Lorentzian line shapes used to extract the full width at half maximum of the peaks. The apparent slightly raised background above 50 MHz is caused by a small ^{167}Er hypefine peak in this region. Data above 50 MHz were not included in the fit to avoid any bias from this. The intensity scale is the voltage measured on a 10^9-V/A transimpedance amplifier connected to the photodiode fluorescence detector.

cence spectrum then permitted correlation of sweep time with laser frequency.

In obtaining the conversion from laser scan voltage to laser frequency via the Fabry-Perot spectrum analyzer, a differential method was used to reduce errors that could result from drift of the laser and/or piezoelectric element in the analyzer. The analyzer was scanned continuously and the spectrum was observed on an oscilloscope. The time interval corresponding to the free spectral range (and hence a laser frequency shift of 1.5 GHz) was thereby determined to be 3.1 ± 0.1 ms. The laser scan voltage was then alternated between +9.5 V (the maximum value) and a series of values

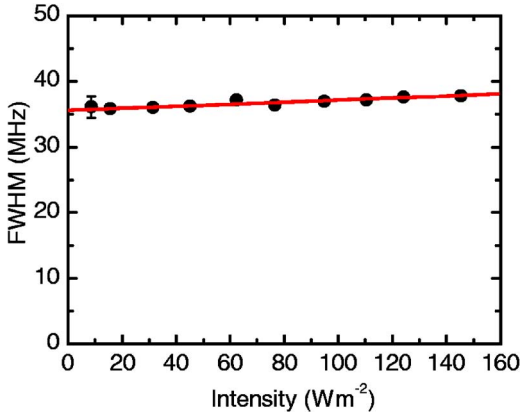

FIG. 2. (Color online) Full width at half maximum peak widths extracted from the data shown in Fig. 1, as a function of incident laser intensity. Measurements are indicated by filled circles, with uncertainties smaller than the symbol size in all cases except the lowest intensity, where an error bar indicates the uncertainty. Solid line (red online) indicates the straight line used to extrapolate to a zero-intensity linewidth value.

TABLE I. Estimates of uncertainty contributions (one standard deviation) to the linewidth measurement of 35.6 MHz derived from the data shown in Figs. 1 and 2. All contributions besides the laser scan calibration are essentially negligible. Note the Doppler width (3.3 MHz) and the laser linewidth ($\approx$2 MHz) add in quadrature to the measured linewidth and hence contribute only a very small broadening.

Source	Uncertainty (MHz)
Laser scan calibration	±1.2
Drift of laser during scan	+0.26
Extrapolation to zero intensity	±0.12
Detector response time	+0.1
Doppler width	+0.1
Laser linewidth	+0.06

that decreased in increments of 1 V. For each voltage value, the shift of the spectrum (in ms) relative to the position at +9.5 V was recorded. Plotting these shifts as a function of voltage yielded a straight line, from which a slope of 0.03771 ± 0.00029 ms V^{-1} was obtained by least-squares fit ($R=0.9995$). The resulting laser scan calibration was 18.26 MHz V^{-1}.

The uncertainty in the linewidth measurement derives from a number of sources, summarized in Table I. The predominant source of uncertainty is the calibration of the laser scan, which is affected by the uncertainties in (a) the free spectral range of the Fabry-Perot analyzer; (b) the ability to measure a time interval between peaks in the swept spectrum analyzer in the presence of laser and/or Fabry-Perot frequency drift; (c) the ability to identify the exact peak positions in the spectrum analyzer; (d) the ability to measure the shift of the spectrum analyzer peak per volt of laser scan voltage; and (e) the linearity of the laser voltage ramp. Further sources of uncertainty include (a) a possible drift of the laser during a measurement, which was estimated by ancillary measurements to be about 0.04 MHz s^{-1}; (b) the uncertainty of the extrapolation to zero intensity (cf. Fig. 2); (c) the finite response time of the fluorescence detector, which causes a broadening of the peak; (d) a residual amount of Doppler spread arising from the diverging atom beam; and (e) the linewidth of the laser, which is convoluted with the measured peak.

Provided that all experimental broadening mechanisms have been accounted for and deemed negligible, the linewidth $\Delta\nu$ measured in the present work is directly related to the lifetime of the excited state by $\tau=(2\pi\Delta\nu)^{-1}$. The lifetime can be used to determine the transition rate by taking its inverse, as long as there are no other significant decay channels from the excited state. In the present case this is a good assumption because no other strong lines in the Er I spectrum have been identified as having the $4f^{12}(^3H_6)6s6p(^1P_1^o)\ (6,1)_7^o$ state as the upper level. The transition rate derived from the present work is thus 2.2×10^8 s^{-1}, a value that differs significantly from the value of 1.73×10^8 s^{-1} reported in the most recent data compilation [4].

The compiled value of the transition rate derives from a review article by Morton [6], which in turn cites a review by

TABLE II. Summary of measurements and calculations of the transition rate A for the $4f^{12}6s^2(^3H_6) \rightarrow 4f^{12}(^3H_6)6s6p(^1P_1{}^o)\ (6,1)_7{}^o$ transition in Er I. Also shown are the lifetime τ, the linewidth $\Delta\nu$, and the oscillator strength f, all of which are simply related to the transition rate (see text). The quantity in italics in each case is the primary value reported; other values are derived.

		A (10^8 s^{-1})	τ (ns)	$\Delta\nu$ (MHz)	f
Compiled value (Ref. [4])		*1.73*	5.8	28	0.48
Experiments	Present work	2.2	4.5	*35.6±1.2*	0.62
	Ref. [8]	1.75	*5.7*	28	0.49
	Ref. [9]	2.6	3.9	41	*0.71*
Calculations	Ref. [10]	*4.76*	2.10	75.7	1.32
	Ref. [11]	2.31	4.32	36.8	*0.643*
	Ref. [2]	2.5	*4.0*	40	0.70

Komarovskii [7] and measurements by Gorshkov and Komarovskii [8]. The review by Komarovskii also cites the measurements of Gorshkov and Komarovskii, and additionally cites measurements by Dohnalik *et al.* [9]. Further input into the transition rate value was obtained from the theoretical calculations of Cowan [10] and Migdalek and Marcinek [11]. Table II summarizes the previous measurements and calculations in comparison with the present result, and also shows the result of a recent calculation based on the relativistic Hartree-Fock code of Cowan [12]. To facilitate comparison, the lifetime $\tau=1/A$, the natural linewidth $\Delta\nu=A/(2\pi)$ and the oscillator strength [13] $f=A(g_2/g_1)\varepsilon_0 m\lambda^2/(2\pi e^2)$ are all shown in addition to the transition rate A.

From Table II, it is clear that the compiled value of the transition rate relies on somewhat sparse, conflicting experimental results. The two previous measurements of A differ from each other by nearly 50%, making a clear determination difficult. The calculations do not provide much guidance either, because they also differ from each other and from the experimental results by large amounts. The present measurement puts the transition rate for this transition on a much firmer basis. The earlier measurements were done by multichannel delayed coincidence and absorption spectroscopy, both of which can be subject to artifacts and can sometimes be difficult to interpret. The crossed-beam laser-induced fluorescence technique used in the present work is much less subject to errors, provided sufficient collimation of the atom beam is ensured and power broadening is addressed. It is further encouraging that the more modern relativistic Hartree-Fock calculation produced a transition rate that agrees well with the experimental result, and at least one of the earlier calculations, using model potentials, also agrees well.

In conclusion, a determination of the transition rate for the $4f^{12}6s^2(^3H_6) \rightarrow 4f^{12}(^3H_6)6s6p(^1P_1{}^o)\ (6,1)_7{}^o$ transition in Er I has been carried out and the value differs significantly from the literature value. Now that an accurate value of this transition rate has been obtained, a wide range of laser cooling experiments utilizing Er can proceed with a firm foundation.

The author wishes to thank J. L. Hanssen, E. Dakin, and J. Reader for valuable discussions relating to this work.

[1] H. J. Metcalf and P. van der Straten, *Laser Cooling and Trapping* (Springer, New York, 1999).

[2] H. Y. Ban, M. Jacka, J. L. Hanssen, J. Reader, and J. J. McClelland, Opt. Express **13**, 3185 (2005).

[3] J. J. McClelland and J. L. Hanssen, Phys. Rev. Lett. **96**, 143005 (2006).

[4] J. E. Sansonetti and W. C. Martin, "Handbook of basic atomic spectroscopic data," http://physics.nist.gov/PhysRefData/Handbook/Tables/erbiumtable3.htm

[5] Unless otherwise noted, all uncertainty estimates are intended to be interpreted as one standard deviation combined standard uncertainty.

[6] D. C. Morton, Astrophys. J., Suppl. Ser. **130**, 403 (2000).

[7] V. A. Komarovskii, Opt. Spektrosk. **71**, 559 (1991) [Opt. Spectrosc. **71**, 322 (1991)].

[8] V. N. Gorshkov and V. A. Komarovskii, Opt. Spektrosk. **50**, 853 (1981) [Opt. Spectrosc. **50**, 467 (1981)].

[9] A. Dohnalik, T. Dohnalik, and M. Szynarowska, Phys. Scr. **20**, 39 (1979).

[10] R. D. Cowan, Nucl. Instrum. Methods **110**, 173 (1973).

[11] J. Migdalek and R. Marcinek, J. Quant. Spectrosc. Radiat. Transf. **32**, 269 (1984).

[12] R. D. Cowan, *The Theory of Atomic Structure and Spectra* (University of California Press, Berkeley, CA, 1981); Cowan programs RCN, RCN2, and RCG.

[13] g_2 is the degeneracy of the excited state, g_1 is the degeneracy of the ground state, ε_0 is the electric constant, m is the electron mass, λ is the vacuum wavelength of the light, and e is the electric charge.